Original Article

The Small Polyphenolic Molecule Kaempferol Increases Cellular Energy Expenditure and Thyroid Hormone Activation

Wagner S. da-Silva,[1] John W. Harney,[1] Brian W. Kim,[1] Jing Li,[1] Suzy D.C. Bianco,[1] Alessandra Crescenzi,[2] Marcelo A. Christoffolete,[1] Stephen A. Huang,[2] and Antonio C. Bianco[1]

Disturbances in energy homeostasis can result in obesity and other metabolic diseases. Here we report a metabolic pathway present in normal human skeletal muscle myoblasts that is activated by the small polyphenolic molecule kaempferol (KPF). Treatment with KPF leads to an ~30% increase in skeletal myocyte oxygen consumption. The mechanism involves a several-fold increase in cyclic AMP (cAMP) generation and protein kinase A activation, and the effect of KPF can be mimicked via treatment with dibutyryl cAMP. Microarray and real-time PCR studies identified a set of metabolically relevant genes influenced by KPF including peroxisome proliferator–activated receptor γ coactivator-1α, carnitine palmitoyl transferase-1, mitochondrial transcription factor 1, citrate synthase, and uncoupling protein-3, although KPF itself is not a direct mitochondrial uncoupler. The cAMP-responsive gene for type 2 iodothyronine deiodinase (D2), an intracellular enzyme that activates thyroid hormone (T3) for the nucleus, is approximately threefold upregulated by KPF; furthermore, the activity half-life for D2 is dramatically and selectively increased as well. The net effect is an ~10-fold stimulation of D2 activity as measured in cell sonicates, with a concurrent increase of ~2.6-fold in the rate of T3 production, which persists even 24 h after KPF has been removed from the system. The effects of KPF on D2 are independent of sirtuin activation and only weakly reproduced by other small polyphenolic molecules such as quercetin and fisetin. These data document a novel mechanism by which a xenobiotic-activated pathway can regulate metabolically important genes as well as thyroid hormone activation and thus may influence metabolic control in humans. *Diabetes* 56:767–776, 2007

From the [1]Division of Endocrinology, Diabetes, and Hypertension, Department of Medicine, Brigham and Women's Hospital, Harvard Medical School, Boston, Massachusetts; and the [2]Tupper Research Institute and Department of Medicine, Children's Hospital Boston, Boston, Massachusetts.

Address correspondence and reprint requests to Antonio C. Bianco, MD, PhD, Brigham and Women's Hospital, 77 Avenue Louis Pasteur, HIM Bldg. #643, Boston, MA 02115. E-mail: abianco@partners.org.

Received for publication 26 October 2006 and accepted in revised form 20 November 2006.

Additional information for this article can be found in an online appendix at http://dx.doi.org/10.2337/db06-1488.

cAMP, cyclic AMP; D1, type 1 deiodinase; D2, type 2 deiodinase; FCCP, carbonyl cyanide p-trifluoromethoxyphenylhydrazone; HEK, human embryonic kidney; HSM, human skeletal muscle; KPF, kaempferol; MSTO, mesothelioma; mt-TFA, mitochondrial transcription factor 1; OCR, oxygen consumption rate; PGC-1α, peroxisome proliferator–activated receptor γ coactivator 1α; PKA, protein kinase A; RMS, rabdomyosarcoma; UCP, uncoupling protein; USP, ubiquitin-specific peptidase; VDU, von Hippel-Lindau protein-interacting deubiquitinating enzyme; WSB-1, suppressor of cytokine signaling [SOCS] box-containing WD-40 protein.

DOI: 10.2337/db06-1488

Molecules that increase energy expenditure are hard to find. Aside from direct mitochondrial uncouplers, thyroid hormone is the most potent substance known to rapidly increase oxygen consumption (1). Recently, it has been reported that dietary supplementation with bile acids confers resistance to diet-induced obesity via upregulation of thyroid hormone signaling in brown adipose tissue. The mechanism in this case involves binding of bile acids to the plasma membrane G protein–coupled receptor TGR-5, which increases cyclic AMP formation and subsequently expression of the gene encoding the thyroid hormone–activating type 2 deiodinase (D2) (2).

Given the discovery that bile acids can regulate energy expenditure and thyroid hormone activation via changes in D2 expression, we have begun to search for nutritional signals that could similarly alter energy expenditure. Our approach has included a screen of potential xenobiotic molecules, i.e., small molecules from plants that trigger biological effects in other organisms, for the ability to increase D2 activity. D2 activity and thyroid hormone T3 production in intact cells were selected as surrogates for induction of the metabolic rate because D2 induction is known to be part of a thermogenic program in brown adipocytes (3) and because D2-mediated T3 production in certain settings could directly contribute to energy expenditure (2). Furthermore, methods for measurement of D2 activity and T3 production are easily performed and could be easily scaled up for screening studies.

Here we report our findings involving kaempferol (KPF), a small polyphenolic molecule found in a number of dietary sources (4). Related polyphenlic molecules in the flavonol family have been reported to have multiple xenobiotic effects, including activation of sirtuins (5). The sirtuins are NAD^+-dependent histone deacetylases known to be induced by caloric restriction, which have been suggested to play a role in fat mobilization as well as in insulin secretion (5). Our studies indicate that KPF treatment increases energy expenditure in normal human skeletal muscle (HSM) myoblasts, while altering the expression of a set of metabolically important genes including *Dio2*, the gene for D2. In addition to characterizing the metabolic effects of KPF on HSM myoblasts, the present study explores the mechanisms underlying the stimulation of *Dio2* expression and demonstrates that KPF increases D2-mediated T3 production.

RESEARCH DESIGN AND METHODS

Reagents and materials. Unless otherwise specified, all reagents were purchased from Sigma Chemical (St. Louis, MO) or Calbiochem (La Jolla, CA). Outer ring–labeled T4 (specific activity 4,400 Ci/mmol) was from PerkinElmer (Boston, MA) and always purified on LH-20 columns before use.

Cell cultures. Rat pituitary tumor cells (GH4C1) were grown as previously described (6). Mesothelioma (MSTO [MSTO-211H]), human embryonic kidney (HEK) epithelial (HEK-293), and rabdomyosarcoma (RMS)-13 (RMS-13) cell lines were obtained from American *Type Culture* Collection. RMS-13 cells were grown in RPMI-1640 supplemented with 10% fetal bovine serum, 2 mmol/l glutamine, 50 μg/ml ampicillin, and 50 μg/ml gentamicin. MSTO-211H and HEK-293 cells were grown and maintained in Dulbecco's modified Eagle's medium supplemented with 10% fetal bovine serum. Normal HSM myoblasts were obtained from Cambrex (Walkersville, MD) and cultured according to the manufacturer's instructions using Cambrex-supplied SkGM2 medium. Sodium selenite was added to all cell culture media at a final concentration of 100 nmol/l (7).

Constructs and transfections. FLAG epitope-tagged human D1 and D2 encoding plasmids have been described (8) as well as the von Hippel-Lindau protein-interacting deubiquitinating enzyme-1 (VDU-1)/ubiquitin-specific peptidase (USP)-33 and VDU-2/USP-20 encoding plasmids (9). Firefly luciferase reporter h*dio2* promoter has been described (10). The cyclic AMP responsive element-luciferase plasmid was from BD Biosciences Clontech (Palo Alto, CA). HEK-293 cells were transfected using LipofectAMINE Plus reagents (Invitrogen, Carlsbad, CA). After transfection, KPF or vehicle was added as indicated. Wherever D2 activity was measured, cells were transfected with 0.1 μg FLAG-D2 plasmid; for the Western blot analysis, cells were transfected with 1 μg FLAG-CysD2 plasmid. In all experiments, plasmids encoding the human growth hormone gene (h*GH*) or renilla luciferase were used to control transfection efficiency, as previously described (11). Experiments were performed in triplicate for each condition.

Oxygen consumption rate. Oxygen consumption rate (OCR) was measured in real-time using an XF24 Extracellular Flux Analyzer (Seahorse Bioscience, N. Billerica, MA). In a typical experiment, cells that had been growing in 75T flasks are trypsinized and counted, and then ~50,000 cells are seeded in customized 24-well plates, each with 28 mm^2 surface and containing ~900 μl media. XF24 optical sensors for measuring oxygen concentration are integrated with disposable probes coupled to fiber-optic wave guides. The wave guide delivers light at various excitation wavelengths and transmits a fluorescent signal to the photo detectors. The fibers are coupled through a set of narrow band pass optical filters to separate the wavelengths specific to each probe's excitation and emission characteristics. The oxygen concentration is measured as the quenching of fluorescence from a porphyrin-based fluorophore specific for oxygen imbedded in a polymer at the tip of the disposable cartridge. The probes are contained in a vertically movable probe head that is lowered onto the wells during each measurement cycle. Lowering the probe head, which is parked at 250 μm above the cell monolayer, reduces the volume in which cells are contained to ~7 μl of media. The OCR is then measured during 5 min, after which the probe head is lifted and the cells exposed to fresh media. The cycle is repeated four times at 5-min intervals.

Oxygen consumption in isolated mitochondria from MSTO-211H cells. Mitochondria were isolated from vehicle and KPF-treated MSTO-211H cells as previously described (12). The OCR was monitored using a Clark-type electrode (model 5300A; YSI Bio-Analytical Products, Yellow Springs, OH). Mitochondria (0.15 mg/ml) were studied at 37°C while incubating with 3.0 ml respiration buffer under continuous stirring. Respiration buffer contained 10 mmol/l Tris-HCl, pH 7.4, 0.32 mol/l mannitol, 8 mmol/l inorganic phosphate, 4 mmol/l $MgCl_2$, 0.08 mmol/l EDTA, 1 mmol/l EGTA, 0.2 mg/ml fatty acid–free BSA (13), and 50 μmol/l P^1,P^5-di(adenosine 5′)-pentaphosphate (Ap5A), an adenylate kinase inhibitor. The latter was included in the media in order to prevent changes in ADP due to adenylate kinase activity.

Microarray analysis. HSM myoblasts were treated with either vehicle or 20 μmol/l KPF for 24 h. Total RNA was extracted using TRIzol reagent (Invitrogen) followed by digestion with DNAse I (Invitrogen) and re-extraction with TRIzol. After quantification, ~8 μg total RNA were submitted to microarray analysis at the Dana-Farber Cancer Institute Microarray Core Facility (Boston, MA) using U133 Plus 2.0 Affymetrix chips that contain >47,000 human transcripts. Two independent RNA samples were analyzed for each condition. The raw image DAT data files were initially processed using Affymetrix GeneChip to create CEL files and DNA-Chip Analyzer (dChip version 2005) according to the developer's manual (14). Differences between the expression levels in vehicle and KPF-treated cells were considered only if statically different ($P < 0.05$), regardless of the fold difference between groups.

Biochemical assays

Cyclic AMP measurement. The cyclic AMP (cAMP) content of MSTO-211H cells was measured using an [^{125}I]cAMP commercial radioimmunoassay kit (NEK-033; Perkin Elmer, Shelton, CT) according to the manufacturer's instructions and previously described methods (15).

Deiodinase activity. Type 1 and type 2 deiodinase (D1 or D2) activities were measured as previously described (16). The different cell types were washed with PBS, harvested, and sonicated in 0.25 mol/l sucrose, 100 mmol/l potassium phosphate buffer, 1 mmol/l EDTA, and 10 mmol/l dithiothreitol. Protein concentration was measured by Bradford using BSA as a standard (17). Assay reactions contained cell sonicates plus 0.5 nmol/l [^{125}I]T4 (for D2) or 0.5 μmol/l [^{125}I]rT3 (for D1), 10 mmol/l dithiothreitol (for D1) or 20 mmol/l dithiothreitol (for D2) in potassium phosphate/EDTA buffer in a total volume of 300 μl. For D2 activity, 1 mmol/l propylthiouracil was added to the reaction mixture to inhibit D1 activity.

T4 to T3 conversion in intact cells. The production of ^{125}I from outer ring–labeled T4, specific activity 5,692 μCi/μg, in intact cells was analyzed by measuring the level of ^{125}I in the medium as described and validated elsewhere (16,18,19) with the following modifications: ^{125}I-T4 was added ~8 h before cells were harvested; at the end of the experiment, 300 μl medium was removed, 200 μl horse serum was added, and protein was precipitated by the addition of 100 μl of 50% trichloroacetic acid followed by centrifugation at 12,000*g* for 3 min; 360 μl of the supernatant containing $^{125}I^-$ was counted in a gamma counter (Cobra II; Packard, Meriden, CT) and expressed as the fraction of the total T4 counts minus the nonspecific deiodination in HEK cell lysate (<5% of the total ^{125}I-T4 counts) and corrected for the volume counted (60%) and the 50% reduction in the specific activity relative to T4. The remaining medium was discarded, the cell pellet was sonicated in PE buffer, and the total protein was assayed for activity normalization. Net T3 production is calculated by multiplying the fractional conversion by the free T4 concentration in the media (20 pmol/l) and expressed as fmol · h^{-1} · mg $protein^{-1}$.

Real-time PCR. Total RNA was extracted using TRIzol reagent (Invitrogen) and used to synthesize cyclic DNA (cDNA) using SuperScript First-Strand Synthesis System for RT-PCR (Invitrogen). The RT-PCR was performed as previously described (20) using cyclophilin A as a housekeeping internal control. Standard curves representing 5-point serial dilution of mixed cDNA of the experimental and control groups were analyzed and used as calibrators of the relative quantification of product generated in the exponential phase of the amplification curve. Only the curves with $r^2 > 0.99$ and amplification efficiency between 80 and 100% were used.

Statistical analysis. All data were analyzed using PRISM software (GraphPad Software, San Diego, CA) and are expressed as means ± SEM. One-way ANOVA was used to compare more than two groups, followed by the Student-Newman-Keuls test to detect differences between groups. The Student's *t* test was used to compare the differences between two groups. $P < 0.05$ was used to reject the null hypothesis.

RESULTS

KPF increases cellular energy expenditure. Cellular energy expenditure was studied using a recently developed noninvasive technology through which the OCR for ~50,000 intact cells is measured during repeated 7-min intervals, based on O_2-mediated quenching of fluorescence from a fluorophore-containing ruthenium complex. In this setting, the metabolic effects of KPF were studied in primary cultures of HSM myoblasts treated for 24–72 h with this small polyphenolic molecule. The OCR was significantly accelerated after 24 h (up ~15%) when compared with vehicle-treated cells, reaching an ~30% increase by 72 h of treatment with KPF (Fig. 1*A* and *B*).

To gain insight into the molecular mechanisms triggered by KPF, microarray studies using U133 Plus 2.0 Affymetrix chips containing >47,000 human transcripts were performed in RNA samples obtained from HSM myoblasts treated with KPF for 24 h. Notably, the signal of 741 probes was significantly affected by this treatment, though the magnitude of these changes was in most cases restricted within twofold of controls (Supplementary Fig. 1 [available in an online appendix at http://dx.doi.org/10.2337/db06-1488]). Only 42 transcripts varied outside these limits, but the corresponding genes are not known to be metabolically relevant (Supplementary Table 1). Nonetheless, the limited changes in probe signals served as the basis for a more accurate analysis of metabolically rele-

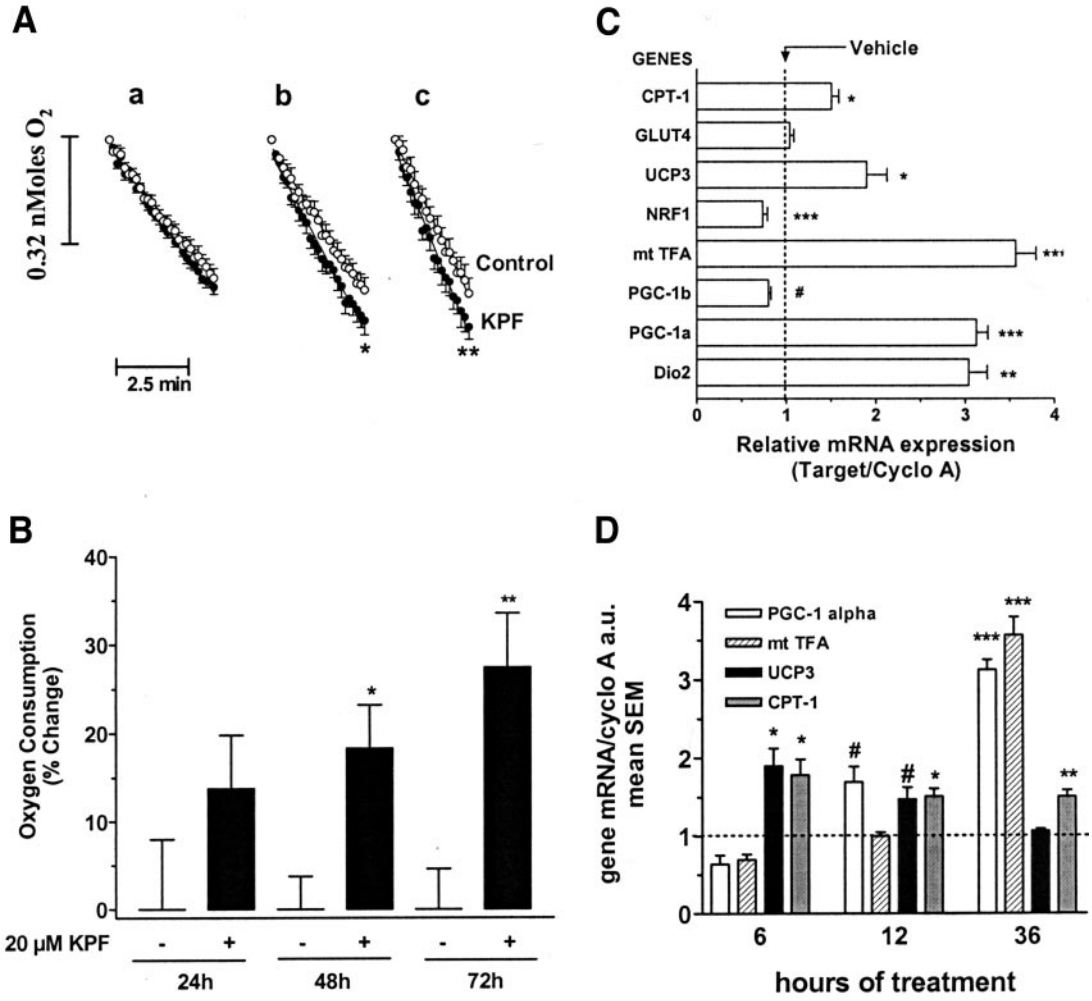

FIG. 1. KPF modifies gene expression and increases energy expenditure. *A*: Real-time measurement of O_2 consumption in intact HSM myoblasts. The cells were treated for 24 (*a*), 48 (*b*), and 72 h (*c*) with 20 μmol/l KPF or vehicle. *B*: Percentage of change in the OCR in cells exposed to 20 μmol/l KPF for 24, 48, and 72 h relative to vehicle-treated cells. *C*: Relative mRNA levels in KPF-treated HSM myoblasts. The changes in gene expression, except for UCP-3 (6 h), were observed after 36 h of treatment. *D*: Time course of changes in mRNA expression in HSM myoblasts treated with 20 μmol/l KPF. *C* and *D*: Dotted line represents relative expression level in vehicle-treated HSM myoblasts normalized to 1. Values are the mean ± SEM of 3–7 samples. #$P < 0.05$, *$P < 0.01$, **$P < 0.001$, ***$P < 0.0001$ compared with vehicle-treated HSM myoblasts.

vant gene expression performed by quantitative RT-PCR, now in cells treated with KPF for 36 h. The expression of five genes was induced by 1.5- to 3.5-fold, including uncoupled protein (UCP)-3, peroxisome proliferator–activated receptor γ coactivator 1α (PGC-1α), carnitine palmitoyl transferase-1, mitochondrial transcription factor 1 (mt-TFA), and *Dio2* (Fig. 1*C*). The time of onset of these changes in mRNA levels varied, but in some cases could be observed as early as 6 h after treatment with KPF (Fig. 1*D*).

Next, we sought to study mitochondria isolated from cells treated with KPF using a Clark electrode setup. To obtain enough cellular material for these experiments, we used a human MSTO cell line (MSTO-211H), which shares the expression of *Dio2* with HSM myoblasts (7) and responsiveness to T3, while exhibiting much higher rates of oxidative phosphorylation. These cells were found to respond to KPF similarly, with 1.2- to 4-fold induction of those same key metabolic genes. In addition, the GLUT4 gene was also upregulated (Fig. 2*A*). In preparations of isolated mitochondria, no changes were observed on the basal succinate oxidation rate (state 2) or in the phosphorylation capacity after the addition of ADP (state 3), indicating that KPF does not stimulate oxidative phosphorylation capacity (Fig. 2*B*). However, mitochondrial uncoupling was fully demonstrated with the use of the uncoupling agent Carbonyl Cyanide P-trifluoromethoxyphenlhydrazone (FCCP). Notably, the acceleration in oxygen consumption by FCCP was greater in mitochondria of KPF-treated cells, indicating enhanced maximal capacity of the respiratory chain (Fig. 2*B*).

KPF modifies metabolic gene expression profile in part by activating the cAMP–protein kinase A pathway. To further understand the mechanism through which KPF modulates gene expression and increases energy expenditure, MSTO-211H cells pretreated for 1 h with eight highly selective signaling inhibitors were exposed to KPF. Only the protein kinase A (PKA) inhibitor H89 was found to prevent the KPF induction of *Dio2* (data not shown). In fact, pretreatment with H89 greatly decreased or completely blocked the 24-h KPF induction of mt-TFA, PGC-1α, and UCP-3 mRNA levels but did not affect the induction of GLUT4 (Fig. 2*A*). This suggests that most of the KPF transcriptional effects depend on the cAMP-PKA pathway, a conclusion further supported by the finding that exposing MSTO-211H cells to dibutyryl cAMP, a stable

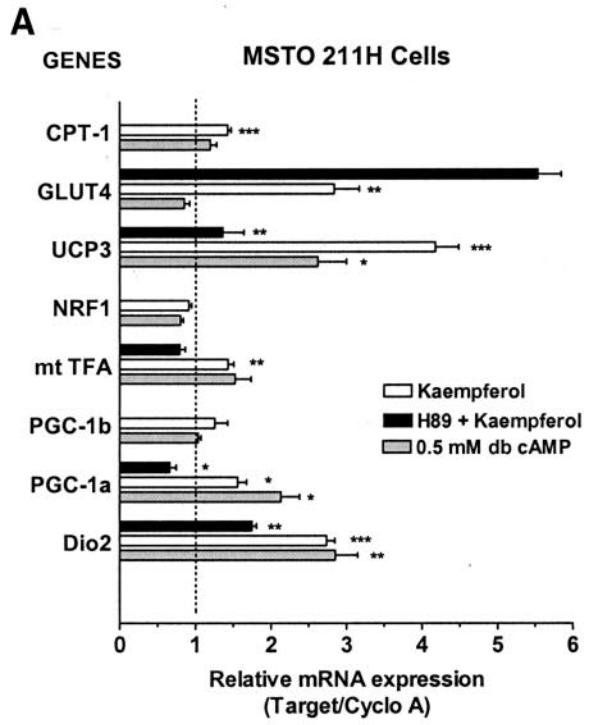

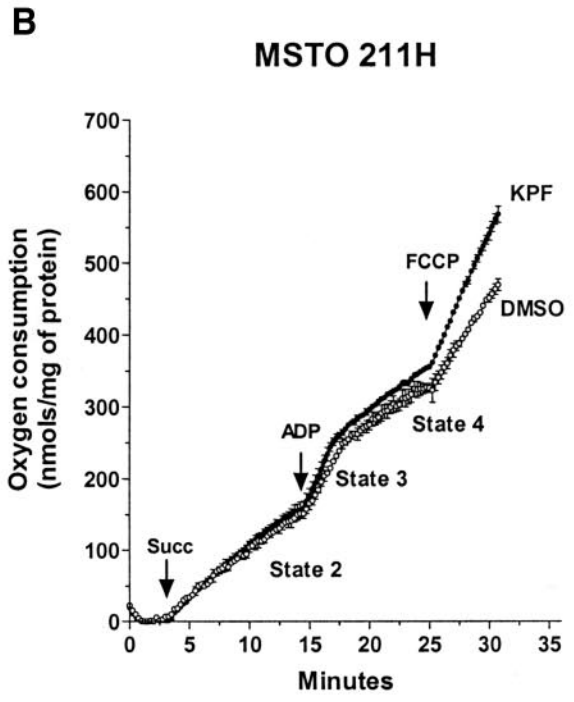

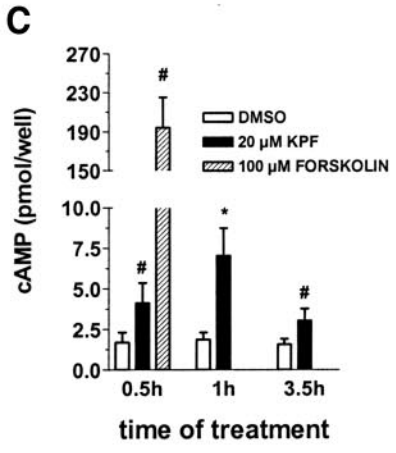

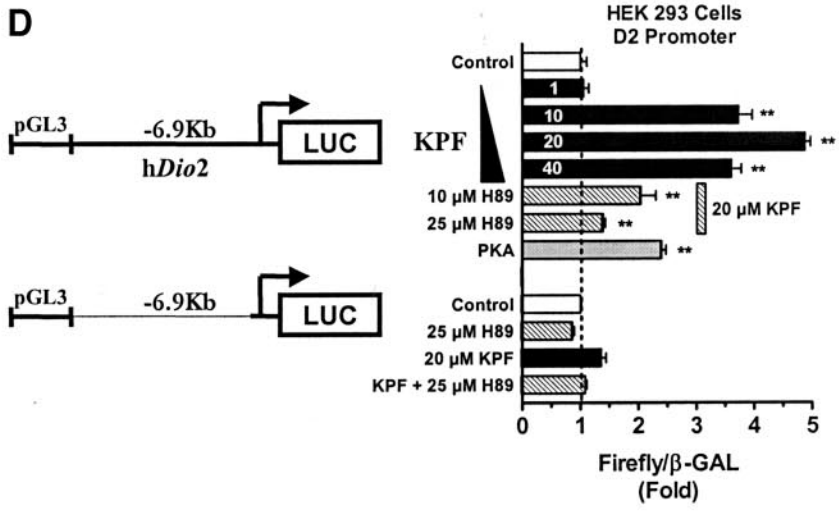

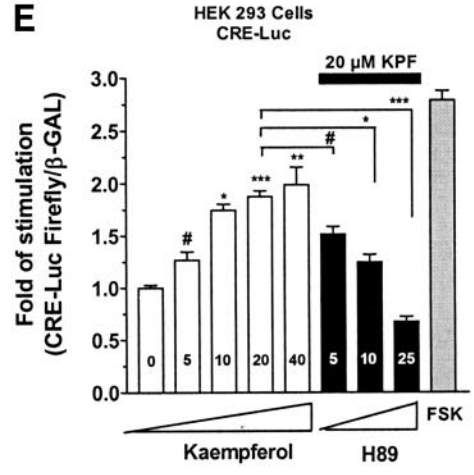

cAMP analogue, for 24 h mimics the gene expression profile produced by KPF (Fig. 2*A*). In fact, the cAMP content of KPF-treated MSTO-211H cells progressively increased 1.9- to 3.8-fold during 30–210 min of incubation (Fig. 2*C*). Activation of this pathway was further supported by findings in HEK-293 cells transiently expressing a cAMP-responsive element–driven reporter gene (CRE-Luc) (Fig. 2*D*). As the *Dio2* promoter is known to have a cAMP-responsive element, HEK-293 cells were transiently transfected with a plasmid containing a Luc reporter driven by a 6.9-Kb *Dio2* 5′ promoter region and treated with KPF (Fig. 2*E*). There was a dose-dependent Luc induction that reached a maximum of approximately five-fold and was blocked by H89, while Luc activity was unaffected by KPF in cells transfected with a *Dio2* promoter-less vector. Finally, to determine how relevant these cAMP-induced changes were for metabolic control, we incubated HSM myoblasts with 0.5 mmol/l dibutyryl cAMP for up to 72 h. This treatment resulted in a progressive acceleration of O_2 consumption, which reached 26 ± 4 and 82 ± 4% above vehicle-treated cells at 48 and 72 h, respectively.

The effects of KPF on D2 induction are weakly reproduced by other small polyphenolic compounds. Focus was then turned to the KPF induction of *Dio2*. D2 is an important component of the thermogenic gene expression profile in stimulated BAT and probably in HSM (3,21–23). First, we verified that *Dio2* induction by KPF resulted in a 8.5- to 50-fold increase in D2 activity in more than one cell line, including HSM myoblasts, MSTO-211H cells, and RMS-13 cells (Fig. 3*A*). Second, the D2 induction was found to be selective with respect to the deiodinase family, since in GH4C1 cells, which constitutively express both D2 and the other T4-activating enzyme, D1, only D2 was stimulated by KPF, while D1 activity was in fact reduced by treatment with this small polyphenolic molecule (Fig. 3*B*). This increase in D2 activity, which is normally quantified by detecting free iodide released during T4 deiodination, was confirmed by a parallel increase in T3 production measured after reaction mixtures were stopped and resolved by high-performance liquid chromatography (Fig. 3*C*), whereas the D2 affinity for T4 remained unchanged (Fig. 3*D*).

Next, we used D2 activity in RMS-13 cells as a readout to screen a large group of natural small polyphenolic molecules that include stilbenes, chalcones, flavones, flavanones, and flavonols and found that only two other flavonols, fisetin and quercetin, were capable of D2 stimulation of up to 3.5- to 5.0-fold (Fig. 3*E*). This indicates that the presence of an OH group at position R3 negatively correlates with D2 stimulating potency within the flavonol group. This difference in potency was also observed while studying time- and concentration-dependency curves (Figs. 3*F* and *G*). Lastly, given that fisetin is a strong activator of the sirtuin pathway (24), we tested whether treatment with other potent sirtuin activators such as resveratrol, piaceatannol, or butein could affect D2 activity. Notably, all three compounds reduced D2 activity level to 25–60% of that of vehicle-treated cells, with resveratrol being the most active in this regard (Table 1). These results indicate that the effects of these small polyphenolic molecules on D2 are not the result of sirtuin activation.

Induction of D2 activity by KPF also involves posttranscriptional mechanisms. It is notable that the induction of D2 mRNA was frequently less prominent than the induction of D2 activity, suggesting that treatment with KPF also induces D2 expression through a posttranscriptional mechanism. To address this possibility, we studied HEK-293 cells transiently expressing D2 with a FLAG peptide tagged to either end of D2. In such cells, D2 protein levels as assessed by Western blotting were markedly elevated after treatment with KPF, while D1 protein levels were unaffected by similar treatment (Fig. 4*A*). To explore this posttranscriptional mechanism further, we then focused on the RMS-13 cells in which the induction of D2 activity by KPF is sizeable (Fig. 3*A*) but the transcriptional effects of KPF less pronounced (data not shown).

Because D2 is known to have a 20-min half-life due to ubiquitination and proteasome degradation, we next tested whether treatment with KPF could interfere with the rates at which D2 is processed through this pathway. Remarkably, in RMS-13 cells the addition of cycloheximide, a commonly used inhibitor of protein synthesis, revealed a dramatically slowed loss of D2 activity of the cells that had been treated with KPF, indicating a prolongation of D2 half-life (Fig. 4*B*). To explore this mechanism further, we first verified that in RMS-13 cells D2 is indeed normally processed by the proteasome system. This in fact is the case, since in other cell lines, treatment with MG132, a specific proteasome inhibitor, increased D2 activity by approximately fourfold (Fig. 4*C*). Next, we tested whether KPF could interfere with D2 uptake by the proteasome complex by combining KPF and MG132 treatments, but this did not seem to be the case (Fig. 4*D*). Furthermore, we observed that the mRNA levels of WSB-1 (suppressor of cytokine signaling [SOC] box-containing WD-40 protein), the D2-specific ubiquitin ligase, and VDU-1/USP33 and VDU-2/USP20, two D2 deubiquitinases, were unaffected by treatment with KPF (Fig. 4*E*). A lack of KPF effects on D2 processing through the ubiquitin-proteasome pathway was also verified in HEK-293 cells (Fig. 4*F–H*). First, we documented that treatment with KPF did not affect the levels of WSB-1, VDU-1/USP33, or VDU-2/USP20 transiently expressed proteins (Fig. 4*F*). Second, WSB-1 knock down also did not interfere with the activity level of transiently expressed D2 (Fig. 4*G*), and, lastly, co-expression of D2 and VDU-1/USP33 did not prevent the KPF effect on D2 activity level, which combined with the results of the other experiments (Fig. 4*A–E*) strongly suggests an alternative pathway for the effects of KPF on D2 half-life.

FIG. 2. KPF increases cAMP concentration. *A*: Gene expression profile in MSTO-211H cells treated for 24 h with 20 μmol/l KPF, pretreated for 2 h with 25 μmol/l H89, the PKA inhibitor, before the addition of 20 μmol/l KPF, and in cells treated with 0.5 mmol/l dibutyryl cAMP. CPT-1, carnitine palmitoyl transferase-1; NRF-1, nuclear respiratory factor 1; PGC-1β, peroxisome proliferator–activated receptor γ coactivator 1β. Dotted line represents relative expression level in vehicle-treated MSTO-211H cells normalized to 1. *B*: Mitochondrial respiratory parameters in isolated mitochondria (450 μg protein) from vehicle-treated (○) and MSTO-211H cells treated with 20 μmol/l KPF for 24 h (●). Succ refers to 2 mmol/l succinate; ADP was used at 0.1 mmol/l and FCCP at 5 μmol/l. *C*: Cellular cAMP production in MSTO-211H cells incubated with KPF or forskolin for the indicated times. *D*: D2 promoter activity as measured by a firefly luciferase (LUC) reporter plasmid in HEK-293 cells treated for 24 h with the indicated concentrations of KPF or H89 or in cells co-expressing the PKA catalytic subunit. *E*: Transcriptional activation of a firefly luciferase reporter plasmid driven by multiple copies of the cAMP-responsive element (CRE)-binding sequence. Cells were treated with the indicated concentrations of KPF or 100 μmol/l forskolin for 24 h. H89 was added 2 h before the addition of KPF. Values are the mean ± SEM of 3–6 samples. #$P < 0.05$, *$P < 0.01$, **$P < 0.001$, ***$P < 0.0001$ compared with vehicle-treated MSTO-211H cells.

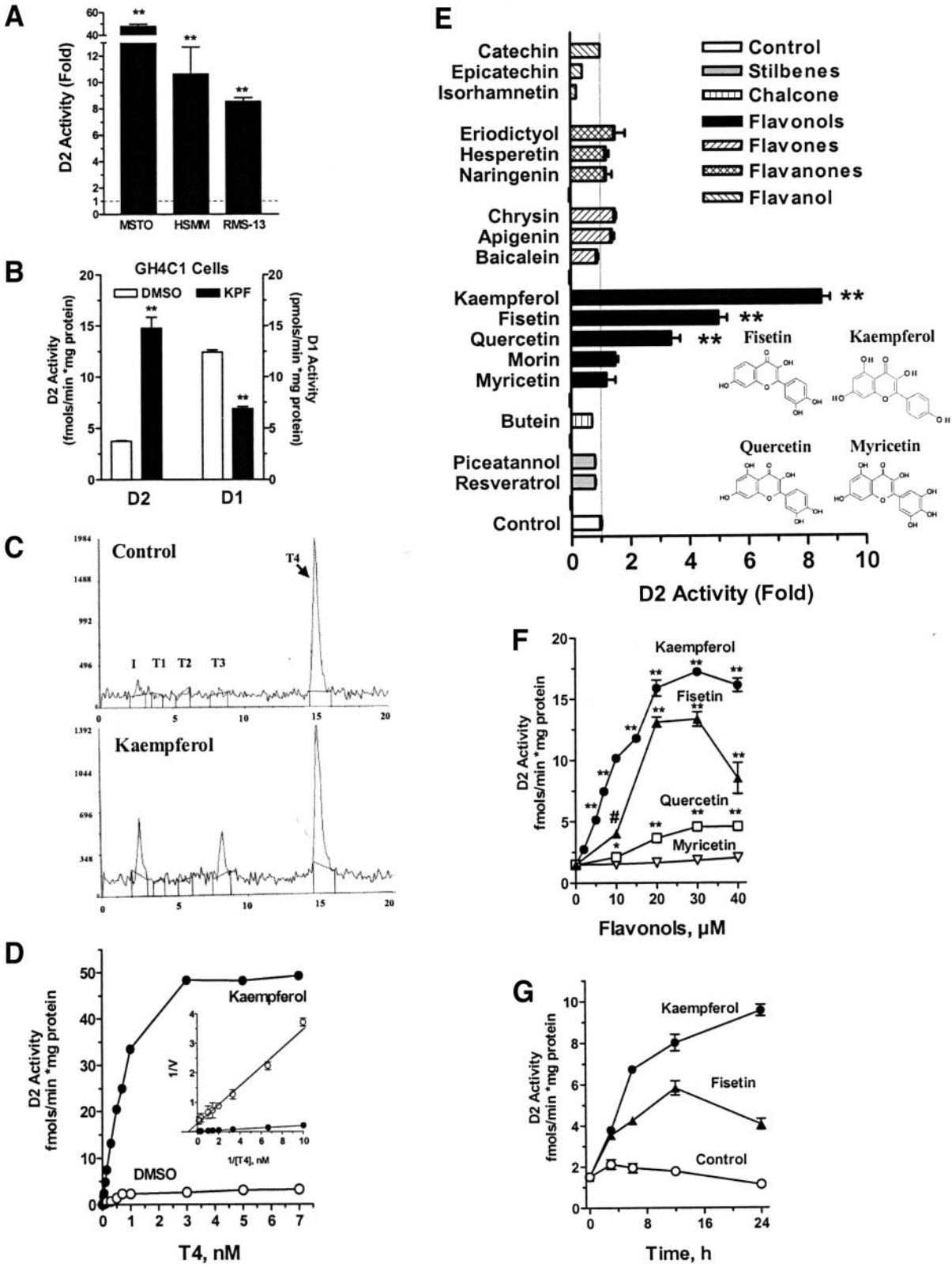

FIG. 3. KPF is a potent stimulator of D2 activity. *A*: D2 activity in MSTO-211H, HSM myoblasts, and RMS-13 cells exposed to 20 μmol/l KPF for 24 h. *B*: Same as in *A* except that D1 and D2 activities were measured in GH4C1 cells. *C*: Cells were treated with 20 μmol/l KPF for 28 h, and sonicates were processed for measuring D2 activity with ^{125I}T4. The reaction products were resolved by reverse-phase high-performance liquid chromatography and the peaks of the indicated iodothyronines identified and quantified by flow radiometry. *D*: Kinetic parameters of D2 in sonicates of cells treated with vehicle (○) or 20 μmol/l KPF (●) for 24 h. *E*: Effects of different dietary polyphenolic compounds on D2 activity in RMS-13 cells. Cells were treated with vehicle or 20 μmol/l of indicated compound for 24 h. Dotted line represents relative activity level in vehicle-treated RMS-13 cells normalized to 1. The chemical structures of the four most potent compounds are also shown. *F*: Dose-response curves of D2 activity in RMS-13 cells treated for 24 h with the indicated amounts of myricetin (▽), KPF (●), Fisetin (▲), or quercetin (□). *G*: D2 activity in RMS-13 cells treated with vehicle (○), 20 μmol/l KPF (●), or 20 μmol/l fisetin (▲) for the indicated times. Values are the mean ± SEM of 3–12 samples. #$P < 0.05$, *$P < 0.01$, **$P < 0.001$, ***$P < 0.0001$ compared with vehicle-treated cells.

TABLE 1
Effects of sirtuin-1 activators on D2 activity

Effect	Treatment (24 h)	D2 Activity (fmol · min^{-1} · mg protein^{-1})
	Control	1.5 ± 0.03 (6)
Activates SIRT1 13.4-fold		
	2 μmol/l Resveratrol	1.8 ± 0.04 (6)*
	5 μmol/l Resveratrol	1.3 ± 0.04 (6)†
	10 μmol/l Resveratrol	1.3 ± 0.04 (6)†
	40 μmol/l Resveratrol	1.0 ± 0.03 (6)‡
	100 μmol/l Resveratrol	0.4 ± 0.01 (6)‡
Activates SIRT1 7.9-fold		
	10 μmol/l Piaceatannol	0.9 ± 0.04 (3)‡
	20 μmol/l Piaceatannol	1.2 ± 0.02 (3)†
	40 μmol/l Piaceatannol	1.3 ± 0.04 (3)*
	100 μmol/l Piaceatannol	0.8 ± 0.04 (3)‡
Activates SIRT1 8.5-fold		
	5 μmol/l Butein	1.4 ± 0.06 (4) NS
	10 μmol/l Butein	1.9 ± 0.05 (4) NS
	20 μmol/l Butein	1.3 ± 0.02 (4) NS
	40 μmol/l Butein	0.9 ± 0.28 (4)*

Data are means ± SEM of 3–6 samples (n). RMS-13 cells were treated with vehicle or the indicated concentrations of resveratrol, piaceatannol, or butein for 24 h. The potency of each molecule on SIRT1 activation is also shown (ref. 24). *$P < 0.05$, †$P < 0.01$, ‡$P < 0.001$. NS, not significant compared with vehicle-treated cells.

KPF-induced T3 production in intact cells. Next, we studied the effect of KPF on deiodination in intact cells, a method by which this process could be examined at physiological cofactor and free T4 concentrations (25).

MSTO-211H cells were incubated with 20 pmol/l free 125I-T4 for ~8 h, and T3 production was calculated based on the free 125I content in the media. Under these conditions, T3 production increased progressively with the concentration of KPF, reaching a maximum of ~2.4-fold stimulation after 48 h of treatment with 7 μmol/l KPF (Fig. 5*A*).

However, this substantial increase in T3 production is lower than would be predicted given the ~50-fold stimulation in D2 activity measured in MSTO-211H cell sonicates (Fig. 3*A*). Furthermore, the increase in T3 production in intact cells is best seen at 48 h of KPF treatment, but the increase in D2 activity in cell sonicates could be seen in as little as 3 h (Fig. 3*F*). Given that D2 protein is clearly increased by KPF treatment (Fig. 4*A*), we next tested the hypothesis that the ability of D2 to catalyze thyroid hormone activation was being impaired to some extent by KPF. T3 production was measured in MSTO-211H cells following 24-h exposure to 10 μmol/l KPF (Fig. 5*B*). Remarkably, KPF washout resulted in a prompt 2.5-fold stimulation of T3 production compared with untreated cells, which peaked ~5 h after KPF washout, and this stimulation persisted >24 h (Fig. 5*B*). These data indicate that while KPF increases D2 enzyme levels, the catalytic ability of the increased D2 is limited such that the increase in T3 production is less than might be expected otherwise.

DISCUSSION

The present studies indicate that KPF can be a potent stimulus of energy expenditure, increasing oxygen consumption in HSM myoblasts significantly at low micromolar concentrations (Fig. 1). The KPF-D2 pathway was found to be consistently operant in a number of different cell lines, allowing us to take advantage of the high oxidative capacity of MSTO-211H cells, the high transfection efficiency of HEK cells, and the minimal transcriptional regulation of D2 in RMS-13 cells in order to dissect out the underlying molecular mechanism. Studies of isolated mitochondria from KPF-treated MSTO-211H cells indicate that KPF does not act as a direct mitochondrial uncoupler (Fig. 2*B*). Instead, its effects result from increased cAMP production (Fig. 2*A* and *C–E*) and induction of a set of metabolically relevant genes (Figs. 1*C* and *D* and Fig. 2*A*). With the exception of GLUT4, the induction of all metabolically relevant genes by KPF can be linked to increased cAMP production and PKA activation (Fig. 2*A*). Indeed, it has been observed previously that KPF increases intracellular cAMP concentrations in colonocytes (26) and uterine smooth myocytes (27), possibly through inhibition of phosphodiesterases (28). While we have no evidence of direct activation of adenylyl cyclases by KPF (data not shown), the structural similarity between KPF and forskolin, also a small polycyclic molecule extracted from plants that directly activates adenylyl cyclase, is notable (29). Ultimately, the potential significance of these findings stems from the identification of this pathway in primary human muscle cells, raising the possibility of therapeutic applications.

A wealth of literature exists regarding possible beneficial effects of KPF and other small polyphenolic molecules, for example in cancer prevention and in the treatment of neurologic and cardiovascular disease (30,31). Furthermore, flavonols have been reported to increase lipolysis (32,33), prompting its addition into many dietary supplements. The current data are novel in that KPF is identified not only as a xenobiotic agent that could increase energy expenditure, but also one that could regulate thyroid hormone activation. However, it must be noted that the KPF concentrations that produced biologic effects seen in this study (2–20 μmol/l) cannot easily be attained via dietary supplementation, since for example ingestion of ~9 mg KPF contained in a cup of endive soup raises serum KPF concentrations to only ~0.1 μmol/l (34). Nevertheless, it is fascinating to speculate as to whether beneficial effects of KPF on human metabolism and thyroid hormone action could be realized if the molecule could be delivered such that plasma levels reached 2 μmol/l, a concentration sufficient to substantially induce D2 activity in our studies. Indeed, considering the potency of KPF treatment on oxygen consumption, with a massive 30% increase seen at 20 μmol/l KPF, it would probably not be necessary to achieve concentrations that high in plasma in order to observe a beneficial therapeutic effect. It is even possible that the changes in gene expression and the stimulation of T3 production following KPF exposure are cumulative.

It is clear from our data that KPF has additional effects beyond its positive cAMP-mediated transcriptional effects (Figs. 2–4). In fact, given that the magnitude of the KPF-induced changes in D2 mRNA is about threefold, the bulk of the increase in D2 activity (up to 50-fold in MSTO-211H cells) must be attributed to the posttranslational effects. D2 can be inactivated via selective ubiquitination but can also be reactivated via deubiquitination, such that proteasomal degradation is not mandatory (6,11). Given that the D2 deubiquitinase VDU-1/USP33 is

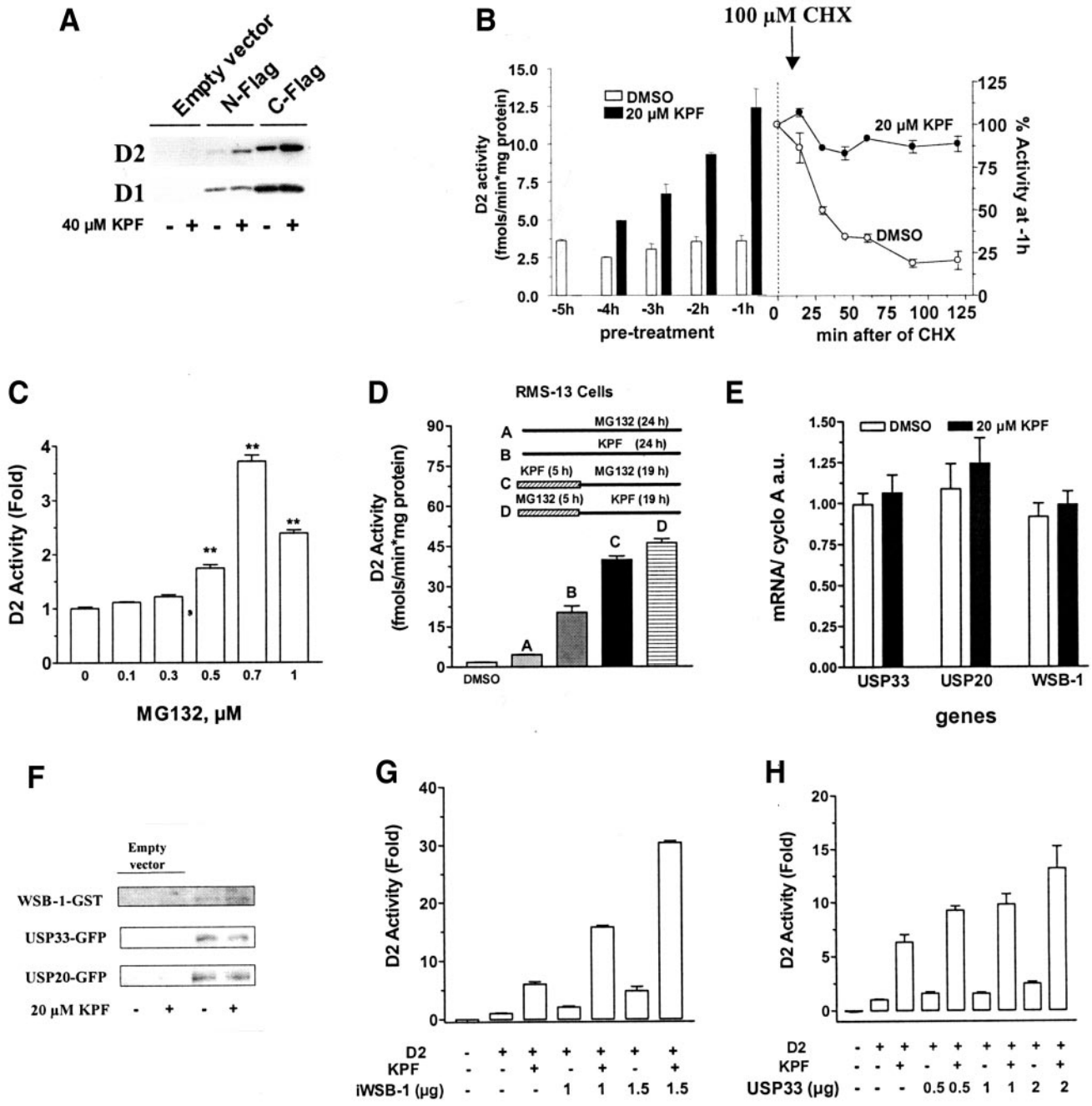

FIG. 4. Posttranscriptional effects of KPF on D2 activity. *A*: Western blot analysis of HEK-293 cells transiently expressing N (amino)- or C (carboxyl)-FLAG-CysD2 and N- or C-FLAG-CysD1. Cells were treated with vehicle or 40 μmol/l KPF for 24 h. Blots were probed with anti-FLAG antibody. *B*: D2 activity in RMS-13 cells treated with 20 μmol/l KPF for 5 h and then exposed to 100 μmol/l cycloheximide to inhibit protein synthesis. *C*: Dose-response curve of D2 activity in RMS-13 cells exposed to the indicated concentrations of MG132; treatment was for 25 h. *D*: D2 Activity in RMS-13 cells treated with 20 μmol/l KPF or 0.7 μmol/l MG132 during the indicated times. *E*: Relative mRNA levels of VDU1/USP33, VDU2/USP20, and WSB-1 in RMS-13 cells treated for 24 h with 20 μmol/l KPF. *F*: Western blot analysis of HEK-293 cells transiently expressing GST–WSB-1, GFP (green fluorescent protein)-USP33, or GFP-USP20 and treated with 20 μmol/l KPF for 24 h. *G* and *H*: D2 activity in HEK-293 cells transiently expressing D2 and iWSB-1 (RNA interference for WSB-1) (*G*) or D2 and VDU1/USP33 (*H*). Indicated in micrograms are the amounts of DNA plasmids transfected. Treatment with 20 μmol/l KPF lasted for 24 h. Values are the mean ± SEM of 3–7 samples. #$P < 0.05$, *$P < 0.01$, **$P < 0.001$, ***$P < 0.0001$ compared with vehicle-treated cells.

cAMP responsive, we explored the possibility that KPF, acting either via cAMP or another pathway, accelerates D2 deubiquitination (9). However, we failed to find a direct connection between KPF and D2 deubiquitination, indicating that another posttranscriptional mechanism exists for regulation of D2 activity (Fig. 4).

Currently, the molecular nature of the posttranslational effects of KPF on D2 remains unclear. While previous reports suggest that very high concentrations of KPF (70 μmol/l) added to cell sonicates inhibit D1 (35), we found no such inhibition of D2 at the concentrations used in this study (data not shown). One possible explanation could be that KPF limits D2 ubiquitination via interference with D2 catalysis, since D2 ubiquitination is accelerated by binding to its substrate (T4). This would explain the discrepancy between the rate of T3 production as measured in

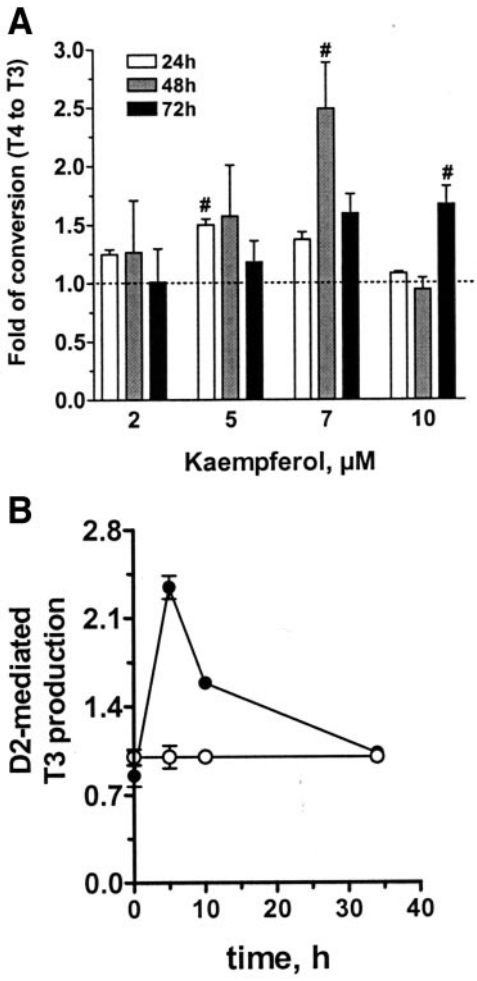

FIG. 5. KPF stimulates T3 production in intact cells. *A*: MSTO-211H cells were treated with the KPF as indicated, and T3 production was measured during the last 8–10 h of treatment. T3 production was calculated based on the free ^{125}I content in the media. Dotted line indicates T3 production in vehicle-treated cells. *B*: Cells were pretreated for 14 h with vehicle (○) or 10 μmol/l KPF (●), and subsequently at time 0 cells underwent a washout with PBS and fresh media without KPF. Values are the mean ± SEM of 3–6 samples. #$P < 0.05$, *$P < 0.01$, **$P < 0.001$, ***$P < 0.0001$ compared with vehicle-treated MSTO-211H cells.

KPF-treated intact MSTO-211H cells, which is increased ~2.4-fold (Fig. 5*A*), versus D2 activity as measured in MSTO-211H cell sonicates, which is increased ~50-fold (Fig. 3*A*). In this regard, KPF has been shown to have pro-oxidative properties, as it induced a concentration-dependent decrease of both the glutathione (GSH) content as well as GSH-S transferase (GST) activity in rat hepatocytes (36), a finding that we confirmed in KPF-treated MSTO-211H cells (data not shown). Thus, it is logical to hypothesize that KPF may limit D2 catalysis in intact cells by somehow interfering with its endogenous thiol cofactor, but confirmation of this hypothesis cannot be completed until the identity of the thiol cofactor is known. In any case, it is clear that KPF does increase D2 enzyme levels (Fig. 4*A*), since T3 production increases further during wash-out of KPF, such that there is a net increase in T3 production both during KPF treatment and even 24 h after exposure to the drug is terminated (Fig. 5).

In summary, the present studies reveal that KPF increases energy expenditure while activating a thermogenic transcriptional program that includes several known metabolically relevant genes, including UCP-3, PGC-1α, carnitine palmitoyl transferase-1, cytrate synthase, mt-TFA, and *Dio2*. Furthermore, KPF has posttranslational effects on D2 that increase its half-life while limiting its ability to catalyze T3-production, creating a pool of D2 enzyme that can mediate increased T3 production, even many hours after KPF is removed from the system. If this KPF metabolic mechanism could be harnessed pharmacologically, a potentially important therapeutic strategy could be realized for the treatment of metabolic disorders.

ACKNOWLEDGMENTS

This study was supported by National Institutes of Health Grants DK65055 and DK64643.

W.S.S. is a fellow of the Pew Charitable Trusts Foundation.

REFERENCES

1. Silva JE: Thermogenic mechanisms and their hormonal regulation. *Physiol Rev* 86:435–464, 2006
2. Watanabe M, Houten SM, Mataki C, Christoffolete MA, Kim BW, Sato H, Messaddeq N, Harney JW, Ezaki O, Kodama T, Schoonjans K, Bianco AC, Auwerx J: Bile acids induce energy expenditure by promoting intracellular thyroid hormone activation. *Nature* 439:484–489, 2006
3. de Jesus LA, Carvalho SD, Ribeiro MO, Schneider M, Kim S-W, Harney JW, Larsen PR, Bianco AC: The type 2 iodothyronine deiodinase is essential for adaptive thermogenesis in brown adipose tissue. *J Clin Invest* 108:1379–1385, 2001
4. Manach C, Scalbert A, Morand C, Remesy C, Jimenez L: Polyphenols: food sources and bioavailability. *Am J Clin Nutr* 79:727–747, 2004
5. Baur JA, Sinclair DA: Therapeutic potential of resveratrol: the in vivo evidence. *Nat Rev Drug Discov* 5:493–506, 2006
6. Steinsapir J, Harney J, Larsen PR: Type 2 iodothyronine deiodinase in rat pituitary tumor cells is inactivated in proteasomes. *J Clin Invest* 102:1895–1899, 1998
7. Curcio C, Baqui MMA, Salvatore D, Rihn BH, Mohr S, Harney JW, Larsen PR, Bianco AC: The human type 2 iodothyronine deiodinase is a selenoprotein highly expressed in a mesothelioma cell line. *J Biol Chem* 276:30183–30187, 2001
8. Curcio-Morelli C, Gereben B, Zavacki AM, Kim BW, Huang S, Harney JW, Larsen PR, Bianco AC: In vivo dimerization of types 1, 2, and 3 iodothyronine selenodeiodinases. *Endocrinology* 144:3438–3443, 2003
9. Curcio-Morelli C, Zavacki AM, Christofollete M, Gereben B, de Freitas BC, Harney JW, Li Z, Wu G, Bianco AC: Deubiquitination of type 2 iodothyronine deiodinase by von Hippel-Lindau protein-interacting deubiquitinating enzymes regulates thyroid hormone activation. *J Clin Invest* 112:189–196, 2003
10. Fekete C, Gereben B, Doleschall M, Harney JW, Dora JM, Bianco AC, Sarkar S, Liposits Z, Rand W, Emerson C, Kacskovics I, Larsen PR, Lechan RM: Lipopolysaccharide induces type 2 iodothyronine deiodinase in the mediobasal hypothalamus: implications for the nonthyroidal illness syndrome. *Endocrinology* 145:1649–1655, 2004
11. Gereben B, Goncalves C, Harney JW, Larsen PR, Bianco AC: Selective proteolysis of human type 2 deiodinase: a novel ubiquitin-proteasomal mediated mechanism for regulation of hormone activation. *Mol Endocrinol* 14:1697–1708, 2000
12. *Mitochondria: A Practical Approach.* Rickwood D, Wilson MT, Darley-Usmar VM, Eds. Washington, D.C., IRL Press, 1987
13. da-Silva WS, Gomez-Puyou A, de Gomez-Puyou MT, Moreno-Sanchez R, De Felice FG, de Meis L, Oliveira MF, Galina A: Mitochondrial bound hexokinase activity as a preventive antioxidant defense: steady-state ADP formation as a regulatory mechanism of membrane potential and reactive oxygen species generation in mitochondria. *J Biol Chem* 279:39846–39855, 2004
14. Li C, Wong WH: Model-based analysis of oligonucleotide arrays: expression index computation and outlier detection. *Proc Natl Acad Sci U S A* 98:31–36, 2001
15. Carvalho-Bianco SD, Kim B, Harney JW, Bianco AC, Mende U, Larsen PR: Chronic cardiac-specific thyrotoxicosis increases myocardial beta-adrenergic responsiveness. *Mol Endocrinol* 18:1840–1849, 2004
16. Christoffolete MA, Ribeiro R, Singru P, Fekete C, da Silva WS, Gordon DF, Huang SA, Crescenzi A, Harney JW, Ridgway EC, Larsen PR, Lechan RM, Bianco AC: Atypical expression of type 2 iodothyronine deiodinase in

thyrotrophs explains the thyroxine-mediated pituitary TSH feedback mechanism. *Endocrinology* 147:1735–1743, 2006
17. Bradford MM: A rapid and sensitive method for the quantitation of microgram quantities of protein utilizing the principle of protein-dye binding. *Anal Biochem* 72:248–254, 1976
18. Buettner C, Harney JW, Larsen PR: The role of selenocysteine 133 in catalysis by the human type 2 iodothyronine deiodinase. *Endocrinology* 141:4606–4612, 2000
19. Croteau W, Bodwell JE, Richardson JM, St Germain DL: Conserved cysteines in the type 1 deiodinase selenoprotein are not essential for catalytic activity. *J Biol Chem* 273:25230–25236, 1998
20. Christoffolete MA, Linardi CCG, de Jesus LA, Ebina KN, Carvalho SD, Ribeiro MO, Rabelo R, Curcio C, Martins L, Kimura ET, Bianco AC: Mice with targeted disruption of the Dio2 gene have cold-induced overexpression of uncoupling protein 1 gene but fail to increase brown adiose tissue lipogenesis and adaptive thermogenesis. *Diabetes* 53:577–584, 2004
21. Scheidegger K, O'Connell M, Robbins DC, Danforth E Jr: Effects of chronic beta-receptor stimulation on sympathetic nervous system activity, energy expenditure, and thyroid hormones. *J Clin Endocrinol Metab* 58:895–903, 1984
22. Mentuccia D, Proietti-Pannunzi L, Tanner K, Bacci V, Pollin TI, Poehlman ET, Shuldiner AR, Celi FS: Association between a novel variant of the human type 2 deiodinase gene Thr92Ala and insulin resistance: evidence of interaction with the Trp64Arg variant of the β-3-adrenergic receptor. *Diabetes* 51:880–883, 2002
23. al-Adsani H, Hoffer LJ, Silva JE: Resting energy expenditure is sensitive to small dose changes in patients on chronic thyroid hormone replacement. *J Clin Endocrinol Metab* 82:1118–1125, 1997
24. Howitz KT, Bitterman KJ, Cohen HY, Lamming DW, Lavu S, Wood JG, Zipkin RE, Chung P, Kisielewski A, Zhang LL, Scherer B, Sinclair DA: Small molecule activators of sirtuins extend Saccharomyces cerevisiae lifespan. *Nature* 425:191–196, 2003
25. Luiza Maia A, Kim BW, Huang SA, Harney JW, Larsen PR: Type 2 iodothyronine deiodinase is the major source of plasma T(3) in euthyroid humans. *J Clin Invest* 115:2524–2533, 2005
26. Nguyen TD, Canada AT, Heintz GG, Gettys TW, Cohn JA: Stimulation of secretion by the T84 colonic epithelial cell line with dietary flavonols. *Biochem Pharmacol* 41:1879–1886, 1991
27. Revuelta MP, Hidalgo A, Cantabrana B: Involvement of cAMP and beta-adrenoceptors in the relaxing effect elicited by flavonoids on rat uterine smooth muscle. *J Auton Pharmacol* 19:353–358, 1999
28. Peluso MR: Flavonoids attenuate cardiovascular disease, inhibit phosphodiesterase, and modulate lipid homeostasis in adipose tissue and liver. *Exp Biol Med (Maywood)* 231:1287–1299, 2006
29. Seamon KB, Padgett W, Daly JW: Forskolin: unique diterpene activator of adenylate cyclase in membranes and in intact cells. *Proc Natl Acad Sci U S A* 78:3363–3367, 1981
30. Grassi D, Necozione S, Lippi C, Croce G, Valeri L, Pasqualetti P, Desideri G, Blumberg JB, Ferri C: Cocoa reduces blood pressure and insulin resistance and improves endothelium-dependent vasodilation in hypertensives. *Hypertension* 46:398–405, 2005
31. Manach C, Mazur A, Scalbert A: Polyphenols and prevention of cardiovascular diseases. *Curr Opin Lipidol* 16:77–84, 2005
32. Kuppusamy UR, Das NP: Effects of flavonoids on cyclic AMP phosphodiesterase and lipid mobilization in rat adipocytes. *Biochem Pharmacol* 44:1307–1315, 1992
33. Kuppusamy UR, Das NP: Potentiation of beta-adrenoceptor agonist-mediated lipolysis by quercetin and fisetin in isolated rat adipocytes. *Biochem Pharmacol* 47:521–529, 1994
34. DuPont MS, Day AJ, Bennett RN, Mellon FA, Kroon PA: Absorption of kaempferol from endive, a source of kaempferol-3-glucuronide, in humans. *Eur J Clin Nutr* 58:947–954, 2004
35. Ferreira AC, Lisboa PC, Oliveira KJ, Lima LP, Barros IA, Carvalho DP: Inhibition of thyroid type 1 deiodinase activity by flavonoids. *Food Chem Toxicol* 40:913–917, 2002
36. Sahu SC, Gray GC: Pro-oxidant activity of flavonoids: effects on glutathione and glutathione S-transferase in isolated rat liver nuclei. *Cancer Lett* 104:193–196, 1996